Influence of specific mechanical energy during compounding in a co-kneader on electrical and rheological properties of multiscale composite materials

Axel Salinier, Sylvie Dagréou, Arthur Visse, Nuria Navascués, Frédéric Léonardi, Christophe Derail

Composites Communications 17 (2020) 154–162

Contents lists available at ScienceDirect

Composites Communications

journal homepage: www.elsevier.com/locate/coco

Short Communication

Influence of specific mechanical energy during compounding in a co-kneader on electrical and rheological properties of multiscale composite materials

Axel Salinier [a,c], Sylvie Dagréou [a], Arthur Visse [a], Nuria Navascués [b], Frédéric Léonardi [a], Christophe Derail [a,*]

[a] CNRS/ UNIV Pau & Pays Adour/ E2S-UPPA, Institut Des Sciences Analytiques et de Physico-Chimie Pour l'Environnement et les Materiaux (IPREM), UMR5254, 64000, Pau, France
[b] Instituto De Nanociencia De Aragón, Universidad De Zaragoza, Calle Mariano Esquillor, Edificio I+D, 50018, Zaragoza, Spain
[c] Plateforme Canoe, Avenue de l'Universite, BP576, 64012, Pau, France

ARTICLE INFO

Keywords:
Composite materials
Multiwalled carbon nanotubes
poly(etherimide)
Co-kneading
Rheology
Electrical threshold
Polymer

ABSTRACT

This paper focuses on the effect of different scales of fillers, from nano to macrometer, on the rheological and electrical behaviour of thermoplastic-based composites. Composites based on poly (etherimide) matrix (PEI) with multiscale reinforcement are processed by melting in a co-kneader to disperse homogeneously carbon nanotubes and glass fibers. We clearly demonstrate the strong link between the liquid-solid transition and the electrical conductivity. We show that the specific mechanical energy is a key parameter. Glass fibers allow to increase the electrical conductivity of blends based on carbon nanotubes and to obtain a lower decreasing of conductivity at the liquid transition which takes place in the same time as rheological and electrical parameters.

1. Introduction

Polymer-based composites are materials of choice for many industrial sectors such as automotive, aeronautics, nautical or energy production industries. Lightweight, strength and easy processing are the main properties that push forward the constantly increasing use of composites. If thermoset matrices have been widely used in composites for several decades, cutting edge research is engaged in the development of the use of new thermoplastic matrices, which are widely seen to be the future of composites, since they have competitive advantages over the thermoset ones, such as better recyclability, subsequent reshaping and weldability.

However, composite materials have limits, such as their poor electrical conductivity. A way to overcome the composites drawbacks and to match the challenges of more demanding specifications is to use nanoparticles as additives in the thermoplastic matrix, in order to confer them additional properties. The composites fabricated with these nanofilled thermoplastic matrices are called multiscale composite materials (MCM) or hierarchical composites, as they contain two types of reinforcements with very different length scales: the conventional reinforcements, usually long fibres, micrometric short fibres or particles; and the nanofillers.

MCM with thermoplastic matrices have been the subject of research in the past years. Recent articles [1,2] give a review of the subject. One objective of adding nanofillers is to improve the mechanical properties. In order to do so, clays [3–9] and carbon nanotubes [10–16] are the most commonly used nanofillers, together with graphene [17] and zirconium oxide [18]. The combined use of micro and nanofillers usually enhances the mechanical properties, the microfillers providing the main mechanical reinforcement, while the nanofillers amplifies it, with a synergetic effect [12,17–19]. In particular, Yang et al. [17] showed that the addition of graphene to poly (arylene ether nitrile)/carbon fibres composites considerably enhances the flexion and fracture behaviour of the composite; TEM micrographs allow to show a significant improvement of the adhesion between the matrix and the carbon fibre with the addition of graphene, which leads to better mechanical charge transfer, and explains the increase of the mechanical properties.

Another targeted property of MCM is the electrical conductivity. It can be obtained by adding electrically conductive nanofillers, such as carbon nanotubes, carbon black or graphene, to conventional

* Corresponding author.
E-mail address: christophe.derail@univ-pau.fr (C. Derail).

https://doi.org/10.1016/j.coco.2019.12.003
Received 13 August 2019; Received in revised form 14 November 2019; Accepted 3 December 2019
Available online 10 December 2019

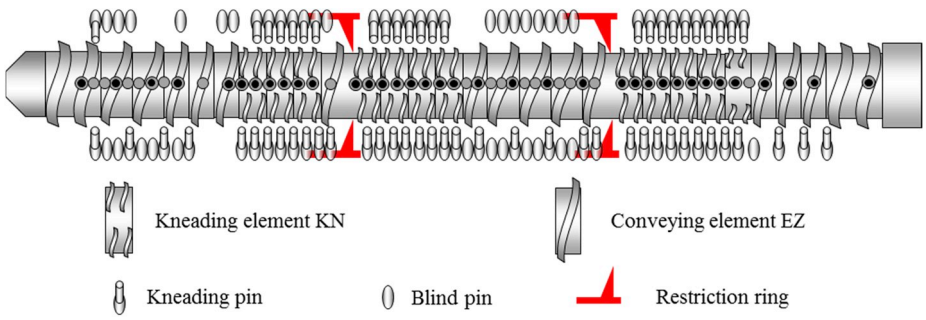

Fig. 1. Screw configuration used to process the different composite materials.

composites. In polymer/glass fibres/carbon nanotubes multiscale composite materials [13,16], the comparison of electrical conductivities with and without glass fibres demonstrated that the presence of electrically isolating glass fibres does not limit the formation of the CNT percolated network. Glass fibres even enhance the electrical properties of the material.

Processing techniques of MCM with thermoplastic matrices are mainly determined by the type and size of micrometric reinforcement. In the case of long, continuous fibres, film stacking of fibre fabrics with films of nanocomposites is the favoured processing method [3,10,11,19–23]. Another possibility to carbon nanotubes in carbon reinforced composites is to graft them on the carbon fibres, before impregnating them with the polymer matrix with conventional processing methods [12,24,25]. When micrometric fillers are short fibres or micro particles, both micro and nanofillers are usually introduced into the thermoplastic matrix by melt compounding [5–8,13–18,26]. Whether to improve mechanical or electrical properties, nanofillers should be well dispersed. When adding nanofillers to enhance the mechanical reinforcement of composites, the existence of agglomerates should be avoided, as it creates points of stress concentration that embrittle the whole material. Conductive nanofillers must form a continuous, percolated network in order to obtain an electrically conductive MCM. The quality of the nanofillers dispersion strongly depends on the processing dispersion. In the case of MCM, the relationship between processing conditions and nanofillers dispersion remains to be studied.

In the present paper, we study poly (ether imide)/glass fibres/carbon nanotubes multiscale composite materials. These materials are melt-processed in a co-kneader. The specific mechanical energy (SME) of the process is varied, by changing the kneader screw speed and feeding rate. In order to understand the role of the presence of the glass fibres in the dispersion of the carbon nanotubes, poly (ether imide)/carbon nanotubes nanocomposites are prepared in the same processing conditions and with the same nanotube content as the MCM. The influence of the SME on both the rheological behaviour and the electrical conductivity is reported. The dispersion of carbon nanotubes is evaluated by transmission electron microscopy. Confrontation of rheological, electrical and morphological properties of MCM, and comparison with the properties of homologous nanocomposites obtained in the same processing conditions, allows to understand the role of glass fibres in the formation of the carbon nanotubes network and suggests a strong relationship between rheology and electrical properties at the liquid-solid transition.

2. Experimental

2.1. Materials

The three commercial grades of PEI used in this study are purchased from SABIC Innovative Plastic with different concentrations of glass fibers (0 wt%: ULTEM 1000, 20 wt%: ULTEM 2200 and 40 wt%: ULTEM 2400). These grades have a Tg of 217 °C. The melt volume rates (MVR) of these grades, measured at 360 °C/5 kg, are 13cm^3/10min, 7cm^3/10min and 5cm^3/10 min, respectively. A masterbatch with 15 wt% of MWCNTs (PEI_15CNT) was purchased from Hyperion catalysis (MB8515-02) in pellet form. The carbon nanotubes used in the masterbatch are generated by decomposition of hydrocarbon gases. They are produced as agglomerates and exist as curled intertwined entanglements [2,3]. Typical diameters range from 10 to 15 nm while lengths are between 1 and 10 μm [27].

Table 1
Composition of each composite in wt%.

Composite Materials	PEI ULTEM 1000	PEI_20 GF ULTEM 2200	PEI_40 GF ULTEM 2400	PEI_15CNT MB8515
PEI_20 GF		100		
PEI_2CNT	86,7			13,3
PEI_20 GF_2CNT		73,4	13,3	13,3

2.2. Melt mixing of composite materials

The concentration of MWCNTs was fixed at 2 wt% for nanocomposites and multiscale composite materials. This concentration was chosen because it is just above the percolation threshold of nanocomposites. This threshold has been evaluated by measuring the evolution of the electrical conductivity as a function of MWCNT content and is equal to 0,85 wt% for pure nanocomposites and 0,98 wt% for multiscale ones.(see supporting data).

All the composite materials were melt blended in a co-kneader (BUSS AG®) having a diameter of 30 mm and L/D = 17. This co-kneader is equipped with a discharge extruder which permits to convey the melt composite, at the end of the kneader part, to the die. The screw configuration is represented in Fig. 1.

All materials were pre-dried at 140 °C during 6 h before blending. Composite materials filled with 20 wt% of glass fibers (ULTEM2200) were melt mixed without any modifications. Nanocomposites materials with 2 wt% of nanotubes were prepared from PEI ULTEM1000 and masterbatch with 15 wt% of MWCNTs. Multiscale composite materials were prepared from masterbatch PEI_15CNT, PEI_20 GF and PEI_40 GF. The PEI_40 GF is used to balance the glass fiber content to obtain, in the multiscale composite materials, 20 wt% of glass fibers. The Table 1 presents the composition of each composite.

Composites, nanocomposites and multiscale composites are prepared for a wide range of mixing conditions, depending on kneader

Table 2
Mixing conditions of nanocomposites and multiscale composite materials.

Feeding rate Q (kg.h^{-1})	Kneader screw speed V_k (rpm)
3	100/200/300/400/500
5	250/300/400/500
6,5	300/400/500

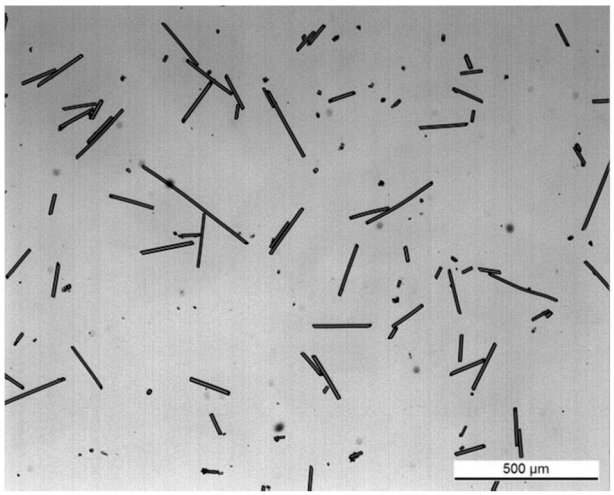

Fig. 2. Example of picture used to evaluate the glass fibers length.

screw speed V_k and feeding rate Q. The temperature barrel is identical for the all conditions and fixed at 400-400-390-390-390 °C for the kneader part, 390 °C for the discharge extruder and 390 °C for the die. The mixing conditions of each kind of composite are listed in Table 2, and for each mixing conditions, specific mechanical energy (SME) is calculated using the Equation (1), where τ is the torque of the kneader (N.m), V_k the screw speed (rpm) and Q the feeding rate (kg.h^{-1}). To calculate the SME, and for the consistency of the units, V_k must be expressed in rad.s^{-1}, and Q in kg.s^{-1}.

$$SME = \frac{\tau . V_k}{Q} \quad \text{Eq.1}$$

2.3. Properties of the composites

2.3.1. Rheological properties

Dynamic mechanical properties of the PEI_CNT nanocomposites and the PEI_20 GF_CNT MCMs were measured using an Advanced Rheometric Expansion System (ARES) oscillatory rheometer (Rheometric Scientific). Plate–plate geometry with a diameter of 10 mm was employed. Prior to the experiments, the samples were dried at 140 °C for 4 h. Solid samples with 10 mm diameter and 2 mm thickness were placed between the preheated plates (350 °C) and were allowed to equilibrate for 5 min. Spectromechanical experiments were performed in the linear viscoelastic domain and in the angular frequency range [10^{-2} – 10^2 QUOTE] *rad.s*$^{-1}$, to determine the viscoelastic behaviour of the samples at low frequencies. All frequency ramps were performed by decreasing frequencies.

All the measurements were performed under nitrogen atmosphere; a fresh sample was used for each spectromechanical experiment.

2.3.2. Electrical properties

The electrical conductivity was determined on extrudate rods using a voltmeter to measure the resistance of the samples. Two meters of extrudate rod were taken off during extrusion. Ten samples of 4 cm length were cut at random locations. The extremities were then metal-coated with a conductive silver paint to enhance the contact between the samples and the voltmeter's electrodes. The volume conductivity using Equation (2) is calculated from measurements of the electrical resistance R (Ω), the length of the specimen L (m) and the cross section S (m^2).

$$\sigma = \frac{L}{S \times R} \quad \text{Eq. 2}$$

2.3.3. Transmission electron microscopy

The morphology of the PEI_CNT nanocomposites and PEI_20 GF_CNT MCMs was observed by transmission electron microscopy. All samples were ultramicrotomed with a diamond knife of Diatome on a Leica EM UC7 microtome at room temperature to give sections with a nominal thickness of 40 nm. The sections were transferred to carbon-coated 150-mesh Cu grids. Bright-field images were obtained at 200 kV with a FEI TECNAI T20 electron microscope (see Fig. 1).

2.3.4. Determination of glass fibers length by optical microscopy

Pellets of composites filled with GF were burned at 550 °C during 5 h to remove the polymer matrix. The GF are then dispersed in a solution of water and glycerol (50 wt%). One droplet of this solution was dropped off on a glass slide to be observed with an optical microscope. Fig. 2 presents an example of picture obtained.

The software ImageJ® was used to analyse the pictures and to quantify L_w and L_n the weight average and number average fiber length

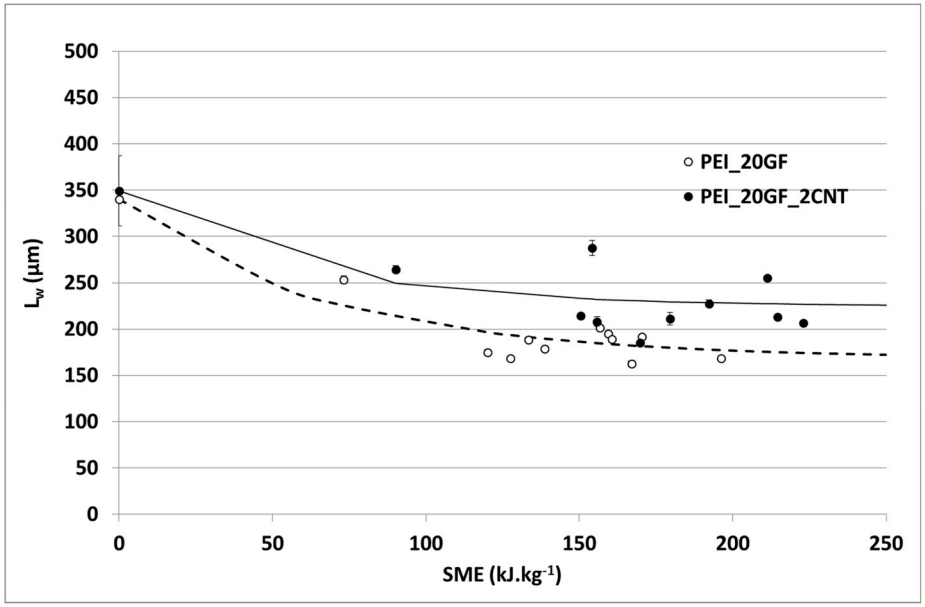

Fig. 3. Evolution of GF length with the specific mechanical energy. Symbols are experimental data and lines are fits by Erreur ! Source du renvoi introuvable.

Table 3
Parameters of the modified Shon-Liu-White model for PEI_20 GF and PEI_20 GF_2CNT.

	L_0 (μm)	L_w (μm)	K''
PEI_20 GF	340 ± 14	163 ± 1	0,015
PEI_20 GF_2CNT	349 ± 38	168 ± 2	0,018

respectively, using the Equation (3), where n_i is the number of fibers of length L_i (μm).

$$L_n = \frac{\sum n_i L_i}{\sum n_i} \quad \frac{\sum n_i L_i^2}{\sum n_i L_i} \qquad \text{Eq. 3}$$

Initial glass fibers length (L_w°) was evaluated by analysing the as-received pellets of PEI_20 GF (ULTEM 2200) and PEI_40 GF (ULTEM 2400) using the method described above. L_w° is determined as (340 ± 14) μm for PEI_20 GF, and $(374 \pm 24) \mu m$ for PEI_40 GF.

3. Results and discussion

3.1. Influence of processing conditions on glass fibers length

Fibers length in short fibers composites is an important parameter which greatly affects the rheological properties as demonstrated by previously studies [4,28].

As the multiscale composite material studied is prepared by mixing of PEI_20 GF and PEI_40 GF, a mixing law writing in Equation (4) was used to determine L_w° from ϕ_{20GF} and ϕ_{40GF} the weight fractions of PEI_20 GF and PEI_40 GF respectively, and L_w^{20GF} and L_w^{40GF} the initial glass fibers lengths of PEI_20 GF and PEI_40 GF respectively.

$$L_w^\circ = \phi_{20GF} \times L_w^{20GF} + \phi_{40GF} \times L_w^{40GF} \qquad \text{Eq. 4}$$

Using **Erreur ! Source du renvoi introuvable.**4, L_w° for PEI_20 GF_2CNT was determined as (349 ± 38) μm.

Several models were developed to describe the evolution of fibers length with processing conditions [29,30]. The modified Shon-Liu-White model, Equation (5), was chosen here. This model is based on L_0 the initial weight average fiber length (μm), L_∞ the final weight average fiber length (μm), K'' the breaking rate constant ($kJ.kg^{-1}$) and SME_{fibers} the specific mechanical energy devoted to the fibers ($kJ.kg^{-1}$).

$$L_w = (L_0 - L_\infty) e^{\left(-K'' \times SME_{fibers}\right)} + L_\infty \qquad \text{Eq. 5}$$

In this study, fibers are introduced as PEI_GF masterbatches in the main hopper of the extruder. We will assume that SME_{fibers} correspond to the total SME.

Evolutions of glass fibers length for PEI_20 GF and PEI_20 GF_2CNT are presented in the Fig. 3.

As can be seen in 3, the GF length strongly decreases during composite processing. For SME higher than 125 $kJ.kg^{-1}$, L_w of PEI_20 GF and PEI_20 GF_2CNT seems to stabilize around 170 μm and 225 μm respectively.

Experimental data are adjusted using Eq. (5). Model parameters for PEI_20 GF and PEI_20 GF_2CNT are listed in the Table 3.

It can be seen in Figure that the modified Shon-Liu-White model gives a good description of the glass fibers length evolution according to the SME. The values of breaking rate constant K″ obtained is the same order of magnitude as the value found by Ville et al. for a co-kneader (0,02) [31] and by Inceoglu et al. for an internal mixer (0,013) [30]. It is also one order of magnitude smaller than the K″ value obtained when using a twin-screw extruder (0.2) [30].

3.2. Influence of processing conditions on the rheological properties of composites

In order to study the influence of processing conditions on the

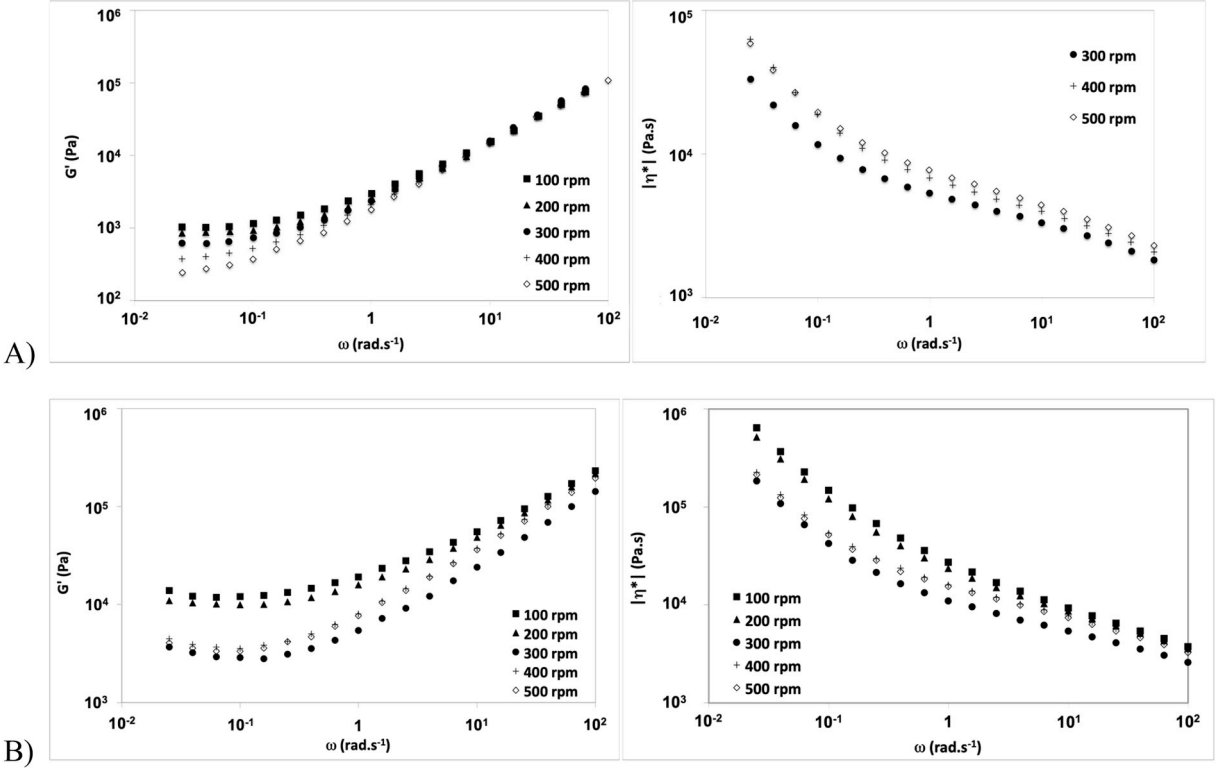

Fig. 4. Evolution of the elastic modulus and of the complex viscosity as a function of the angular frequency for A) PEI_2CNT nanocomposites, and B) PEI_20 GF_2CNT multi-scale composites for different screw speeds, at a feeding rate of 3 kg h^{-1}.

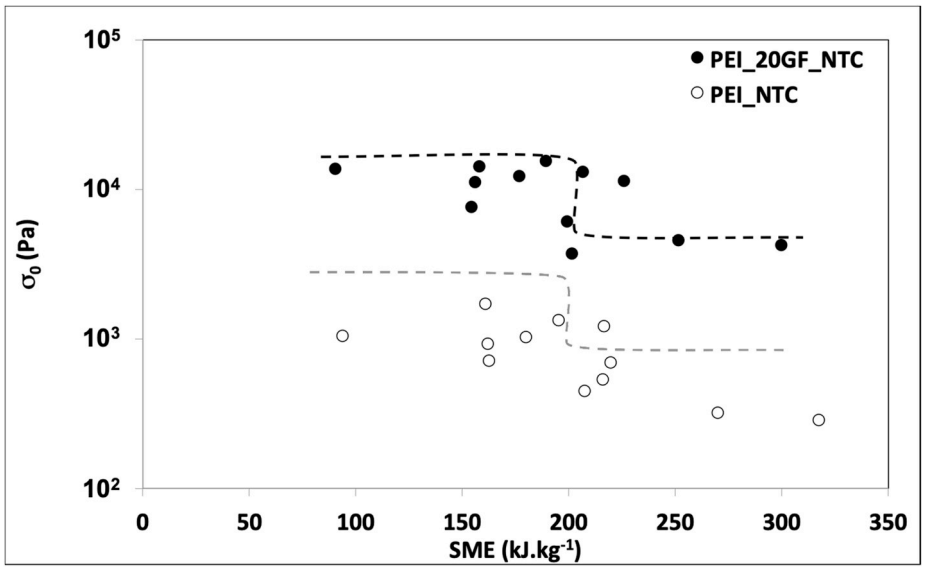

Fig. 5. Yield stress σ_0 calculated from the Cross model as a function of the Specific Mechanical Energy (SME) (dotted line is a guide for the eyes).

rheological behaviour of the prepared composites, we measured the spectromechanical properties of both nanocomposites (PEI_2NTC) and multiscale composites (PEI_20 GF_2NTC), prepared using different kneader feeding rates and screw speeds.

Fig. 4 (A and B) reports the evolution of the storage modulus *G*' and the complex viscosity $|\eta^*|$ as a function of frequency, for nanocomposites (PEI_2NTC) and multiscale composites (PEI_20 GF_2NTC), for one feeding rate as an example ($Q = 3\ kg.h^{-1}$) and various screw speeds. These results are typical of the ones obtained for all the feeding rates.

The rheological behaviour observed for both nanocomposites and multiscale composites is typical of filled polymers in the terminal region of the polymer matrix. Indeed, fillers induce the appearance of a *G*' plateau zone and an increase of $|\eta^*|$ at the lower frequencies. This is related to the formation of a network of fillers, which dominates the rheological behaviour at low frequencies, and prevents the relaxation of the polymer chains [32].

At the lowest frequencies studied, which correspond to the longest experimental times, G′ slightly increases from the plateau behaviour, in particular in the case of PEI_20 GF_2CNT multi-scale composites. In order to relate this phenomenon to the evolution of the material during the experiment, time sweeps were performed at 350 °C. An increase of less than 10% was measured for nanocomposites, while it reached 20% for multiscale materials. This can explain the slight increase in G' observed at low frequencies. This evolution may be attributed either to polymer degradation or to some changes in the state of dispersion of the fillers; this point has not been explored in the present work.

Variations of *G*' and $|\eta^*|$ are directly related to the state of dispersion of the fillers in the polymer matrix [33–36]. An increase of *G*' and $|\eta^*|$ at low frequencies, together with the appearance of a *G*' plateau, are the signature of a more homogeneous fillers' dispersion state in the polymeric matrix. We will thus focus our interest on the variations of *G*' and $|\eta^*|$ at low frequencies as a function of the processing parameters.

For both nanocomposites and multiscale composites, the kneader screw speed has in impact on the state of dispersion of the fillers in the matrix: *G*' and $|\eta^*|$ indeed vary at low frequency.

In the case of nanocomposites (PEI_2NTC), for a $3\ kg.h^{-1}$ feeding rate, we notice the appearance of a plateau for *G*' for all screw speeds. The value of G' for the plateau zone decreases when the screw speed increases, as well as $|\eta^*|$. It thus seems that the state of dispersion is more homogeneous for lower screw speeds. Note that for the highest feeding rate studied ($6,5\ kg.h^{-1}$, results in supporting data 1), the inverse tendency is observed: the CNT dispersion state is more homogeneous for higher screw speeds.

In the case of multiscale composites (PEI_20 GF_2CNT), for a $3\ kg.h^{-1}$ feeding rate, for the lowest screw speeds (100 and 200 *rpm*), *G*' and $|\eta^*|$ have higher values for higher screw speed values, which can be related to a better dispersion state of the fillers. At intermediate feeding rate ($5\ kg.h^{-1}$, results not presented here), no clear tendency could be identified, while for the highest feeding rate ($6,5\ kg.h^{-1}$, results not presented here), the screw speed has no influence on *G*' and $|\eta^*|$.

In order to quantify the influence of the processing parameters on the rheological behaviour of nanocomposite and multiscale composites, the evolution of the complex viscosity $|\eta^*|$ as a function of frequency was modelled. We chose to use a modified Cross model [37] shown in Equation (6) which includes a yield stress term that describes the viscosity increase at low frequencies: this fitting method was already used by Charman et al. to model EPDM/EVA/CNT nanocomposites behavior [38]. The complex viscosity $|\eta^*|$ depends on σ_0 the yield stress, η_0 the zero shear viscosity, τ the mean relaxation time, and n the power law index.

$$|\eta^*(\omega)| = \frac{\sigma_0}{\omega} + \frac{\eta_0}{1+(\tau\omega)^n} \qquad \text{Eq. 6}$$

The value of the yield stress is related to the rheological behaviour at low frequencies. For unfilled polymers, with a Newtonian behavior at low frequencies (characterization by a viscosity plateau), the yield stress value tends to zero. For filled polymers with a solid-like behaviour at low frequencies, the yield stress value increases and can be correlated to the fillers' dispersion state [38].

The parameters of the modified Cross model (σ_0, η_0, τ and n) were adjusted to the experimental data, using a non-linear regression method programed with MatLab®.

Fig. 5 shows the yield stress values for both nanocomposites (PEI_2CNT) and for multi-scale composites (PEI_20 GF_2CNT) as a function of the Specific Mechanical Energy (SME). One can remark σ_0 decreases when the SME increases indicating that.dispersion of fillers is more homogeneous for low SME values for both materials. Increasing the energy provided to the material during processing is unfavorable to the formation of homogeneous fillers' dispersion within the PEI matrix. Moreover, an important decrease of σ_0 is observed for SME values of $(220 \pm 20\ kJ\ kg^{-1})$ for the two composites. This suggests that the state of dispersion of fillers for SME above and below these values is different. The similarity between both values also supports the idea that the presence of glass fibers does not have influence on the dispersion state of

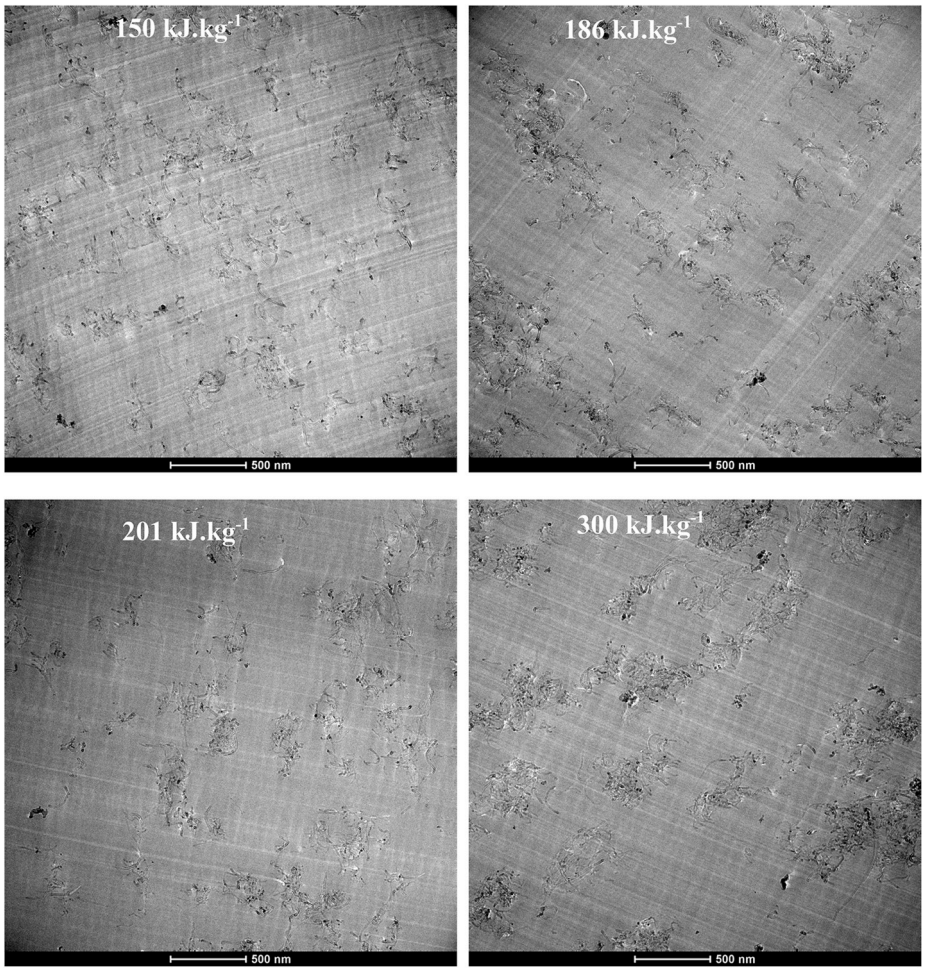

Fig. 6. TEM micrographs of PEI_20 GF_2CNT processed with SMEs of 150; 186; 201 and 300 kJ kg^{-1}.

Table 4
Evolution of the aggregate surface measured on PEI_20 GF_2CNT micrographs with SME.

SME (kJ. kg^{-1})	Mean aggregate surface (nm^2)	Surface standard deviation (nm^2)
150	41 000	21 000
186	44 000	35 000
201	70 000	28 000
300	175 000	72 000

carbon nanotubes which would pilot the dispersion state. This result is in good agreement with previous conclusions obtained on PEI/carbon nanotubes nanocomposites and PEI/glass fibers/carbon nanotubes multi-scale composites, processed by twin-screw extrusion [16] where it was observed that both materials had very similar electrical percolation curves, which means similar dispersion states of conducting carbon nanotubes. We will present electrical analysis in the next part.

In order to visualize the evolution of the CNT network with SME increasing, TEM micrographs were realized on samples processed with different SMEs. Fig. 6 shows the micrographs obtained for PEI_20 GF_2CNT multi-scaled composites. Those obtained for nanocomposites, presented as supporting data 2, are very similar.

It can be seen that for SME values lower than around 200 $kJ.kg^{-1}$, dispersion of CNTs is homogeneous within the PEI matrix. The CNT network is spread and continuous, and occupies a large surface on the micrograph. It seems to be constituted of interconnected small aggregates, which expects a large number of connections between CNTs, glass fibers and polymer chains, and explains large yield stress values. For larger SME values, the CNT network is less spread and discontinuous. It is constituted of isolated agglomerates, with important zones without CNTs.

The surface of aggregates (that is to say, the surface of non-isolated CNTs) appearing on the SEM micrographs were measured using the ImageJ software. Table 4 summarizes the results of these measurements. It can be seen that the aggregates mean size indeed shows an sharp increase for SMEs larger than 200 kJ kg^{-1}, thus confirming the qualitative observation.

The yield stress decrease can thus be attributed to the loss of connections between CNTs, glass fibers and polymer chains.

3.3. Influence of processing conditions on the electrical properties of composites

Conductivity of both PEI_2CNT and PEI_20 GF_2CNT was studied as a function of SME. Results are shown on Fig. 7.

For both materials, a decrease of conductivity is observed, for SME values equal to $(215 \pm 20\ kJ.kg^{-1})$ for both composites. It thus appears that low SME values during processing are more favorable to the formation of a conductive CNT network. It should be noted that these values are very similar, and comparable to the respective SME values of yield stress decrease. This suggests an evident relationship between rheological and electrical properties, related to the evolution of fillers' network structure with SME.

The decrease of electrical conductivity is very sharp in the case of PEI_2CNT nanocomposites, with an electrical conductivity of 10^{-3} *S*.

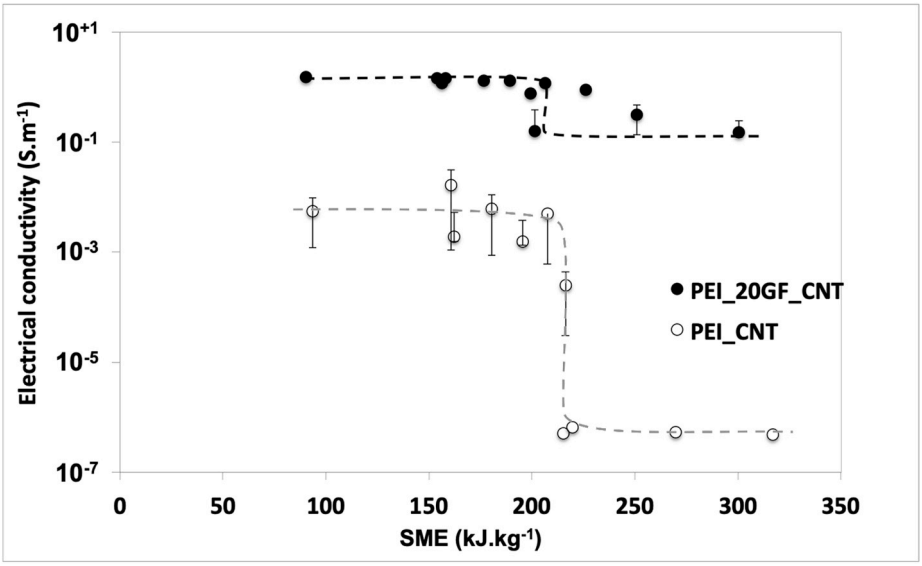

Fig. 7. Electrical conductivity as a function of the Specific Mechanical Energy (SME).

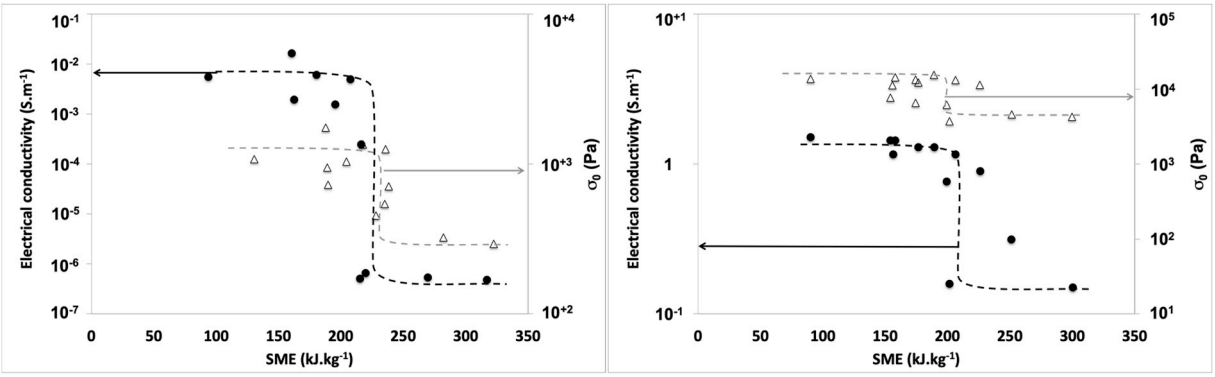

Fig. 8. Comparison of rheological and electrical conductivity as a function of the Specific Mechanical Energy (SME) for PEI_2CNT and PEI_20 GF_2CNT.

m^{-1} for SME values lower than 215 $kJ.kg^{-1}$ falling down to 10^{-7} $S.m^{-1}$ for values above 215 $kJ.kg^{-1}$. This result is in good agreement with what is observed from TEM micrographs: for low SMEs, the CNT network appears widely spread and continuous, with conductive paths allowing electrical current circulation; on the contrary, when SME increases, discontinuities appear in the CNT network, thus interrupting the conductive paths.

Increasing of SME during processing of polymer/CNT nanocomposites reduces the size of CNT aggregates, as demonstrated by Villmow et al. [39] and Pötschke et al. [40] for twin-screw extrusion. As concluded by these authors, this decrease in the agglomerate size at the micrometric scale suggests a better dispersion of CNTs at the nanometric scale. However, the authors show that improving CNT dispersion leads to an increase in *G*' for low SME values, followed by an important decrease for high SMEs [40]. The electrical conductivity values that they measure follow the same trend. Degradation of CNTs with increasing SME, leading to shorter nanotube length, was evidenced. This degradation reduces the probability of contacts between CNTs, and thus the probability for the formation of a percolating network within the polymer matrix.

Our results are in a good agreement with these conclusions and bring an interesting demonstration of the link between rheological and electrical properties for this type of materials. We can therefore make the hypothesis that a reduction of the CNT length with increasing SME explains the evolution of rheological and electrical properties of PEI_CNT

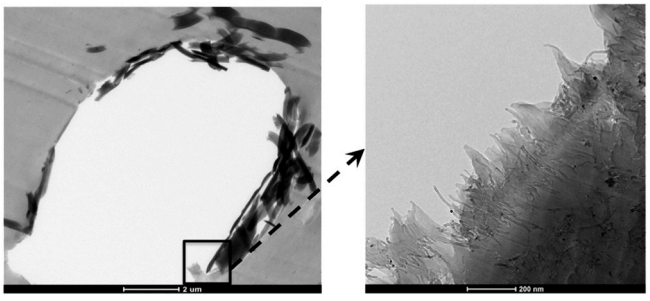

Fig. 9. TEM micrographs of multi-scale composites – Left-hand: location left empty by a glass fiber torn away during ultramicrotome cutting – Right-hand: magnification of the glass fiber surface.

nanocomposites. We can expect that a critical value of SME (at around 200 $kJ.kg^{-1}$) is necessary to degrade CNTs and reduce their length, thus reducing the possibilities of CNT entanglements and contacts, resulting in lower electrical conductivity and lower *G*'.

As a conclusion, we report on the Fig. 8 the electrical and rheological behaviour as a function of SME for the two types of composites. This representation accentuates the link between the two properties and the expected behaviour (see Fig. 9).

When comparing the variation of electrical conductivity of

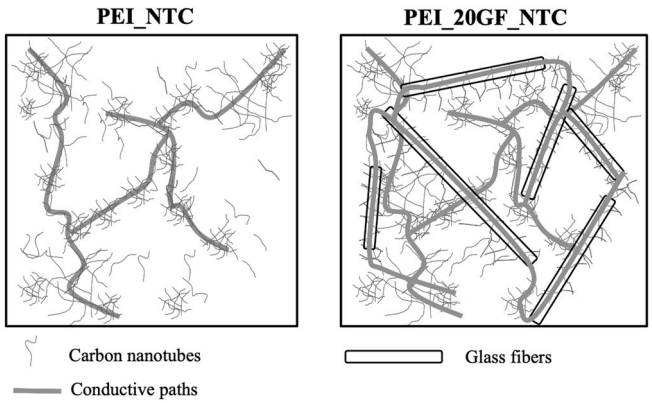

Fig. 10. Scheme of the conductive paths in A) PEI_2CNT nanocomposites and B) PEI_20 GF_2CNT multi-scale composites.

nanocomposites with SME, to the one of multi-scale composite materials (Fig. 8), we first observe that the conductivity of MCM is much higher than the one of nanocomposites. As the electrical conductivity of both nanocomposites and multi-scale composite materials relies on the existence of a percolated network of carbon nanotubes, we studied the architecture of this network in order to explain the highest conductivity of MCM. Fig. 9 presents a TEM micrograph of a sample of PEI_20 GF_2CNT. The left-hand image corresponds to a location left empty by a glass fibers torn away during sample cutting with the ultramicrotome. The right-hand photo is a magnification of the interface between glass fibers and PEI. It can be seen that carbon nanotubes accumulate on that interface, and orientate perpendicular to the glass fibers surface. We can propose a scheme of the preferential location and orientation of carbon nanotubes near the glass fibers surface creates new conductive paths, in addition to the CNT network already existing in nanocomposites (Fig. 10).

When increasing the SME applied to MCM samples, a decrease of electrical conductivity is observed for a critical value (200 $kJ.kg^{-1}$) as in the case of nanocomposites (Fig. 7). This decrease is much less pronounced: above 200 $kJ.kg^{-1}$, the conductivity is reduced by around one order of magnitude with glass fibers, when the reduction is quite 4 orders of magnitude without glass fibers. One can consider that this less pronounced decrease is due to a protective role of the glass fibers towards the CNT percolated network. This can be attributed to the preferential location and orientation of carbon nanotubes near the glass fibers, which prevents the destruction of CNT agglomerates during the extrusion process, and preserves the architecture of the conductive paths.

4. Conclusion

In this paper, we propose a study of multiscale composite materials based on carbon nanotubes and glass fibers dispersed in a polymer matrix at the melting state and by using a co-kneader. This paper demonstrates clearly the strong link between (i) the SME and the quality of the dispersion, (ii) the electrical and rheological behaviour of this type of materials and finally (iii) the link with the structure of nanotubes within the bulk and particularly around the glass fibers. This paper demonstrates the expectations of authors for multiscale composite materials and brings interesting way to predict electrical properties for conductive composites based on thermoplastics and dedicated on aeronautical, automotive applications.

Declaration of competing interest

The authors declare that they have no known competing financial interests or personal relationships that could have appeared to influence the work reported in this paper.

Appendix A. Supplementary data

Supplementary data to this article can be found online at https://doi.org/10.1016/j.coco.2019.12.003.

References

[1] A.M. Díez-Pascual, Hybrid carbon nanotube/fiber thermoplastic composites: mechanical, thermal, and electrical characterization, Hybrid Polym. Compos. Mater. Prop. Characterisation (2017) 169–201, https://doi.org/10.1016/B978-0-08-100787-7.00008-1.
[2] G. Mittal, K.Y. Rhee, V. Mišković-Stanković, D. Hui, Reinforcements in multi-scale polymer composites: processing, properties, and applications, Compos. B Eng. 138 (2018) 122–139, https://doi.org/10.1016/j.compositesb.2017.11.028.
[3] D.P.N. Vlasveld, W. Daud, H.E.N. Bersee, S.J. Picken, Continuous fibre composites with a nanocomposite matrix: improvement of flexural and compressive strength at elevated temperatures, Compos Part Appl Sci Manuf 38 (2007) 730–738, https://doi.org/10.1016/j.compositesa.2006.09.010.
[4] D.-W. Zhang, Y.-J. Li, Y.-H. Feng, J.-P. Qu, H.-Z. He, B.-P. Xu, Effect of initial fiber length on the rheological properties of sisal fiber/polylactic acid composites, Polym. Compos. 32 (2011) 1218–1224, https://doi.org/10.1002/pc.21141.
[5] M.J. Clifford, T. Wan, Fibre reinforced nanocomposites: mechanical properties of PA6/clay and glass fibre/PA6/clay nanocomposites, Polymer 51 (2010) 535–539, https://doi.org/10.1016/j.polymer.2009.11.046.
[6] T. Mohan, K. Kanny, Influence of nanoclay on rheological and mechanical properties of short glass fiber-reinforced polypropylene composites, J. Reinf. Plast. Compos. 30 (2011) 152–160, https://doi.org/10.1177/0731684410391509.
[7] S.-H. Wu, F.-Y. Wang, C.-C.M. Ma, W.-C. Chang, C.-T. Kuo, H.-C. Kuan, et al., Mechanical, thermal and morphological properties of glass fiber and carbon fiber reinforced polyamide-6 and polyamide-6/clay nanocomposites, Mater. Lett. 49 (2001) 327–333, https://doi.org/10.1016/S0167-577X(00)00394-3.
[8] T. Wan, S. Liao, K. Wang, P. Yan, M. Clifford, Multi-scale hybrid polyamide 6 composites reinforced with nano-scale clay and micro-scale short glass fibre, Compos Part Appl Sci Manuf 50 (2013) 31–38, https://doi.org/10.1016/j.compositesa.2013.03.009.
[9] D.P.N. Vlasveld, H.E.N. Bersee, S.J. Picken, Nanocomposite matrix for increased fibre composite strength, Polymer 46 (2005) 10269–10278, https://doi.org/10.1016/j.polymer.2005.08.003.
[10] A.M. Díez-Pascual, B. Ashrafi, M. Naffakh, J.M. González-Domínguez, A. Johnston, B. Simard, et al., Influence of carbon nanotubes on the thermal, electrical and mechanical properties of poly(ether ether ketone)/glass fiber laminates, Carbon 49 (2011) 2817–2833, https://doi.org/10.1016/j.carbon.2011.03.011.
[11] Z. Shen, S. Bateman, D.Y. Wu, P. McMahon, M. Dell'Olio, J. Gotama, The effects of carbon nanotubes on mechanical and thermal properties of woven glass fibre reinforced polyamide-6 nanocomposites, Compos. Sci. Technol. 69 (2009) 239–244, https://doi.org/10.1016/j.compscitech.2008.10.017.
[12] S. Rahmanian, K.S. Thean, A.R. Suraya, M.A. Shazed, M.A. Mohd Salleh, H. M. Yusoff, Carbon and glass hierarchical fibers: influence of carbon nanotubes on tensile, flexural and impact properties of short fiber reinforced composites, Mater. Des. 43 (2013) 10–16, https://doi.org/10.1016/j.matdes.2012.06.025.
[13] N. Gamze Karsli, S. Yesil, A. Aytac, Effect of hybrid carbon nanotube/short glass fiber reinforcement on the properties of polypropylene composites, Compos. B Eng. 63 (2014) 154–160, https://doi.org/10.1016/j.compositesb.2014.04.006.
[14] B. Hornbostel, P. Pötschke, J. Kotz, S. Roth, Mechanical properties of triple composites of polycarbonate, single-walled carbon nanotubes and carbon fibres, Phys E Low-Dimens Syst Nanostructures 40 (2008) 2434–2439, https://doi.org/10.1016/j.physe.2007.08.100.
[15] F. Puch, C. Hopmann, Morphology and tensile properties of unreinforced and short carbon fibre reinforced Nylon 6/multiwalled carbon nanotube-composites, Polymer 55 (2014) 3015–3025, https://doi.org/10.1016/j.polymer.2014.04.052.
[16] A. Salinier, S. Dagréou, F. Léonardi, C. Derail, N. Navacués, Electrical, rheological and mechanical characterization of multiscale composite materials based on poly (etherimide)/short glass fibers/multiwalled carbon nanotubes, Compos. Struct. 102 (2013) 81–89.
[17] X. Yang, Z. Wang, M. Xu, R. Zhao, X. Liu, Dramatic mechanical and thermal increments of thermoplastic composites by multi-scale synergetic reinforcement: carbon fiber and graphene nanoplatelet, Mater. Des. 44 (2013) 74–80, https://doi.org/10.1016/j.matdes.2012.07.051.
[18] G. Lin, G. Xie, G. Sui, R. Yang, Hybrid effect of nanoparticles with carbon fibers on the mechanical and wear properties of polymer composites, Compos. B Eng. 43 (2012) 44–49, https://doi.org/10.1016/j.compositesb.2011.04.029.
[19] W. Yang, Y. Hu, Q. Tai, H. Lu, L. Song, R.K.K. Yuen, Fire and mechanical performance of nanoclay reinforced glass-fiber/PBT composites containing aluminum hypophosphite particles, Compos Part Appl Sci Manuf 42 (2011) 794–800, https://doi.org/10.1016/j.compositesa.2011.03.009.
[20] A.H. Barber, Q. Zhao, H.D. Wagner, C.A. Baillie, Characterization of E-glass–polypropylene interfaces using carbon nanotubes as strain sensors, Compos. Sci. Technol. 64 (2004) 1915–1919, https://doi.org/10.1016/j.compscitech.2004.02.004.
[21] E.A. Stefanescu, X. Tan, Z. Lin, N. Bowler, M.R. Kessler, Multifunctional fiberglass-reinforced PMMA-BaTiO3 structural/dielectric composites, Polymer 52 (2011) 2016–2024, https://doi.org/10.1016/j.polymer.2011.02.050.
[22] B. Ashrafi, A.M. Díez-Pascual, L. Johnson, M. Genest, S. Hind, Y. Martinez-Rubi, et al., Processing and properties of PEEK/glass fiber laminates: effect of addition of

single-walled carbon nanotubes, Compos Part Appl Sci Manuf 43 (2012) 1267–1279, https://doi.org/10.1016/j.compositesa.2012.02.022.
[23] A.M. Díez-Pascual, J.M. González-Domínguez, M. Teresa, M.A. Gómez-Fatou, Poly (ether ether ketone)-based hierarchical composites for tribological applications, Chem. Eng. J. 218 (2013) 285–294, https://doi.org/10.1016/j.cej.2012.12.056.
[24] H. Qian, A. Bismarck, E.S. Greenhalgh, M.S.P. Shaffer, Carbon nanotube grafted carbon fibres: a study of wetting and fibre fragmentation, Compos Part Appl Sci Manuf 41 (2010) 1107–1114, https://doi.org/10.1016/j.compositesa.2010.04.004.
[25] P. Agnihotri, S. Basu, K.K. Kar, Effect of carbon nanotube length and density on the properties of carbon nanotube-coated carbon fiber/polyester composites, Carbon 49 (2011) 3098–3106, https://doi.org/10.1016/j.carbon.2011.03.032.
[26] D.P.N. Vlasveld, P.P. Parlevliet, H.E.N. Bersee, S.J. Picken, Fibre–matrix adhesion in glass-fibre reinforced polyamide-6 silicate nanocomposites, Compos Part Appl Sci Manuf 36 (2005) 1–11, https://doi.org/10.1016/j.compositesa.2004.06.035.
[27] P. Pötschke, T.D. Fornes, D.R. Paul, Rheological behavior of multiwalled carbon nanotubes/polycarbonate composites, Polymer 43 (2002) 3247–3255.
[28] T. Köpplmayr, I. Milosavljevic, M. Aigner, R. Hasslacher, B. Plank, D. Salaberger, et al., Influence of fiber orientation and length distribution on the rheological characterization of glass-fiber-filled polypropylene, Polym. Test. 32 (2013) 535–544, https://doi.org/10.1016/j.polymertesting.2013.02.002.
[29] Y. Shimizu, S. Arai, T. Itoyama, H. Kawamoto, Experimental analysis of the kneading disk region in a co-rotating twin screw extruder: Part 2. glass-fiber degradation during compounding, Adv. Polym. Technol. 16 (1997) 25–32, https://doi.org/10.1002/(SICI)1098-2329(199721)16:1<25::AID-ADV3>3.0.CO;2-L.
[30] F. Inceoglu, J. Ville, N. Ghamri, J.L. Pradel, A. Durin, R. Valette, et al., Correlation between processing conditions and fiber breakage during compounding of glass fiber-reinforced polyamide, Polym. Compos. 32 (2011) 1842–1850, https://doi.org/10.1002/pc.21217.
[31] J. Ville, F. Inceonoglu, F. Ghamri, J.L. Pradel, A. Durin, R. Valette, et al., A study of fiber breakage during compounding in a buss kneader, Int. Polym. Process. 27 (2012) 245–251.
[32] R. Inoubli, S. Dagréou, A. Lapp, L. Billon, J. Peyrelasse, Nanostructure and mechanical properties of polybutylacrylate filled by grafted silica particles, Langmuir 22 (2006) 6683–6689.
[33] Q. Zhang, F. Fang, X. Zhao, Y. Li, M. Zhu, D. Chen, Use of dynamic rheological behavior to estimate the dispersion of carbon nanotubes in carbon nanotube/polymer composites, J Polym Chem B 112 (2008) 12606–12611.
[34] K. Zhou, S.-Y. Gu, Y.-H. Zhang, J. Ren, Effect of dispersion on rheological and mechanical properties of polypropylene/carbon nanotubes nanocomposites, Polym. Eng. Sci. 52 (2012) 1485–1494, https://doi.org/10.1002/pen.23098.
[35] M. Guehenec, V. Tishkova-Leoni, S. Dagréou, F. Léonardi, C. Derail, P. Puech, et al., The effect of twin screw extrusion on structural, electrical, and rheological properties in carbon nanotube poly-ether-ether-ketone nanocomposites, J. Appl. Polym. Sci. 129 (2013) 2527–2535.
[36] F. Du, R.C. Scogna, W. Zhou, S. Brand, J.E. Fischer, K.I. Winey, Nanotube networks in polymer nanocomposites: rheology and electrical conductivity, Macromolecules 37 (2004) 9048–9055.
[37] M. Cross, Rheology of non-Newtonian fluids: a new flow equation for pseudoplastic systems, J. Colloid Sci. 20 (1965) 417–437.
[38] M. Charman, F. Léonardi, S. Dominguez, C. Bissuel, C. Derail, Dispersion of multiwalled carbon nanotubes in a rubber matrix using an internal mixer: effects on rheological and electrical properties, J. Polym. Sci., Part B: Polym. Phys. 49 (2011) 1597–1604, https://doi.org/10.1002/polb.22350.
[39] T. Villmow, B. Kretzschmar, P. Pötschke, Influence of screw configuration, residence time, and specific mechanical energy in twin-screw extrusion of polycaprolactone/multi-walled carbon nanotube composites, Compos. Sci. Technol. 70 (2010) 2045–2055, https://doi.org/10.1016/j.compscitech.2010.07.021.
[40] P. Pötschke, T. Villmow, B. Krause, Melt mixed PCL/MWCNT composites prepared at different rotation speeds: characterization of rheological, thermal, and electrical properties, molecular weight, MWCNT macrodispersion, and MWCNT length distribution, Polymer 54 (2013) 3071–3078, https://doi.org/10.1016/j.polymer.2013.04.012.